ADVANCES IN THE SLAC RDDS: MODELING MANIFOLD DAMPING AND ITS EFFECT ON THE WAKEFIELD FOR THE NEXT LINEAR COLLIDER

R.M. Jones; SLAC, N. M. Kroll; UCSD & SLAC, RH. Miller,
T.O. Raubenheimer and R.D. Ruth; SLAC

Abstract

The RDDS (Rounded Damped Detuned Structure) accelerator damps the transverse wakefield excited by bunches of electrons traversing thousands of linear accelerator structures. Errors in the fabrication of the cells which constitute each structure can result in a wakefield which is resonantly driven by the bunches, leading to BBU (Beam Break Up) and to a substantial growth in the beam emittance. One means to avoid these deleterious effects is to provide additional damping of the manifold, via plating the walls of the manifold with an electrically lossy material such as canthol or by fabricating the wall with stainless steel rather than copper. Results are presented on the wakefield and emittance growth in structures with a moderately lossy manifold.

1 INTRODUCTION

The SLAC damped detuned accelerator structures (the DDS and RDDS series) provide moderate damping of the transverse wakefields by means of four waveguide-like damping manifolds that run the length of the structure, gathering dipole excitation energy from the individual accelerator cells and conveying it to termination assemblies at each end of the structure, where it is

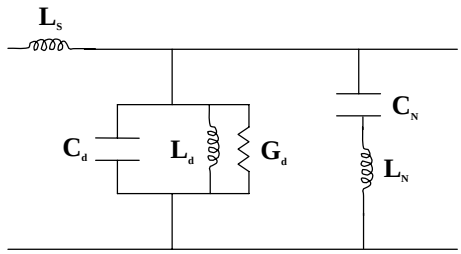

Figure 1: Transmission Line Model of Manifold

absorbed and may also be detected [1]. The damping manifolds also act as pumping manifolds and, via spectral analysis of the detected radiation, as beam position monitors. The equivalent circuit model [2], which has been a primary design tool for these structures, has so far neglected the absorption of energy in the walls of the manifolds. In this paper we modify the equivalent circuit so as to include these effects and explore the effects of both normal (i.e. copper) losses and losses enhanced by the use of lossier materials in the walls. The impact of including internal losses in the equivalent circuit theory spectral function (or wake impedance) analysis has already been discussed in the context of cell losses in [3], and the analysis given there applies equally well here.

2 THE EQUIVALENT CIRCUIT MODEL OF MANIFOLD DAMPING

As described in [2], the manifold is modeled as a transmission line periodically shunted with a localized susceptance. The distributed series reactance per unit length and the distributed shunt susceptance per unit length are chosen so as to give the wave impedance and propagation characteristics of a TE waveguide mode. The dispersion relation for the manifold is given by

$$\cos\phi = \cos\phi_0 - \tfrac{1}{2} B_s \, z \sin\phi_0 \qquad (2.1)$$

Here ϕ_0 is the phase advance for one structure period P of the transmission line, z the frequency f dependent characteristic impedance of the line, and B_s the localized P spaced shunt susceptances. In our modelling B_s has been represented by an L-C series resonant circuit with capacitance C_s and resonant frequency F_m, yielding the explicit form:

$$\cos\phi = \cos\phi_0 - \alpha \, (\pi P f / c)^2 \; F_m^2/(F_m^2 - f^2) \, \mathrm{sinc}\phi_0 \qquad (2.2)$$

Note that $\cos\phi$ is a single valued analytic function of ϕ_0^2 rather than its double valued square root, with $\phi_0^2 = (2\pi P/c)^2 \left(f^2 - F_c^2\right)$, where F_c is the cutoff frequency of the transmission line section. Apart from that of ϕ_0 all frequency dependencies in (2.2) are shown explicitly, and α is a dimensionless constant proportional to C_s. The propagation characteristics of the loss-less manifold are thus fully characterized by the parameters α, F_m, and F_c, and may be determined for individual cells from the uniform structure dispersion relations obtained by simulation as described in [2], and their cell to cell variation is determined by the same procedures as are used for all of the other equivalent circuit parameters.

We model manifold attenuation by adding a distributed shunt conductance G_d to the distributed shunt susceptance,

$2\pi f C_d \left(1 - F_c^2 / f^2\right)$, where C_d is the distributed capacitance per unit length. This leads to:

$$\phi_0^2 \rightarrow \left(2\pi P / c\right)^2 \left(f^2 - F_c^2 - jfF_c / Q_m\right) \qquad (2.3)$$

where we have expressed G_d as a manifold Q_m via $G_d = 2\pi C_d F_c / Q_m$. Alternative representations of transmission line loss were considered but rejected because they led to undesirable analytic behaviour in the complex frequency plane. This occurs well outside of the frequency range of interest and would probably have had no practical significance, but it seemed preferable to avoid it. Inserting the modification represented by (2.3) into (2.2) yields for small Q_m^{-1}, $\cos\phi \rightarrow \cos\phi - j\xi Q_m^{-1}$, which, in the same limit, yields a cell-to-cell fractional amplitude decrease $\xi(1/Q_m)/\sin\phi$. Here ξ is a parameter easily determined from Eq. (2.2). As described in [2], the parameterisation of the equivalent circuit model is based upon simulation of a small number of fiducial cells treated as uniform structures with cell-to-cell parameter variation for the remaining cells obtained by an interpolation procedure [4]. These same simulations can be used to compute a perturbative wall loss Q_w for the manifold mode mode branch of the simulation. The corresponding cell-to-cell amplitude decrease is $\frac{1}{2} f d\phi/df/Q_w$. Equating the two expressions for the cell-to-cell amplitude decrease yields:

$$Q_m = 2Q_w \sin\phi / (\xi f d\phi / df) \qquad (2.4)$$

In determining Q_w for some individual cell+manifold section from a simulation, one applies periodic boundary conditions to the section with a specified phase advance. Away from avoided crossing regions (see [2]) the manifold mode is easily identified and well represented by Eq. (2.2). Where this is the case the effect of the coupling of the manifold to the cells, omitted in Eq. (2.2) is sm all, and Q_w may be computed from the simulated fields in the usual way. In the determination of Q_m from Eq. (2.4), the frequency f is determined from the simulation, while $\sin\phi$, $d\phi/df$, and ξ are determined from Eq. (2.2). (Q_w may depend somewhat upon the frequency and phase advance at which it is determined. Eq. (2.4) holds strictly when the phase advance is specified such that f = F_c) Computations so far carried out yield 4500 as a representative value of Q_w, from which one obtains 4200 as a representative value for Q_m.

3 WAKEFIELD REDUCTION AND EMITTANCE PRESERVATION

RDDS1 is the current version of the KEK/SLAC accelerator which damps the transverse wakefields. In fabricating the structure, 4 cells have been decoupled from the manifold at either end of the accelerator (prompted by mechanical design considerations) and the fundamental mode coupler loads down the downstream end of the accelerator to the extent that the Q of the last cell is 36. Both of these effects are included in the simulation of the wakefield (shown in Fig 2), together with the finite reflection from the higher order mode coupler in the manifold. However, in bonding the cells an error occurred in the geometry of the middle cells such that their radius increased by approximately 20 μm but the implications of this will not be reported here [5].

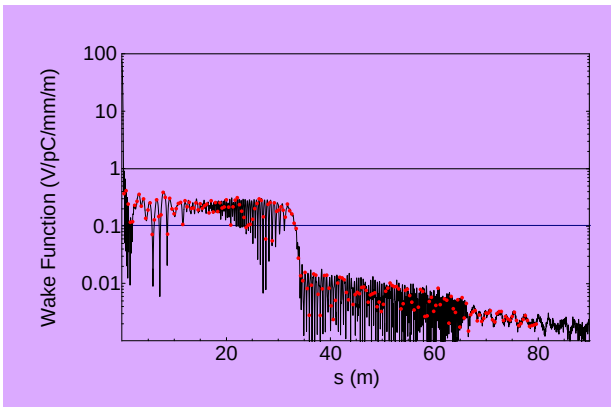

Figure 2: Envelope of Wakefunction with Q ~ Q $_{copper}$

The sum wake at a particular bunch is defined as the wake that is left behind by all preceding bunches, and it provides a measure of how large the emittance growth it likely to be. In Fig 3 the RMS deviation of the sum wakefield from the mean value for RDDS1 is shown as a function of a small change in the spacing of the bunches (this is a convenient way to change the synchronous frequency of the cells). The nominal bunch spacing (84 cm) is close to a minimum in the sum wakefield and hence emittance growth is unlikely to be a problem for

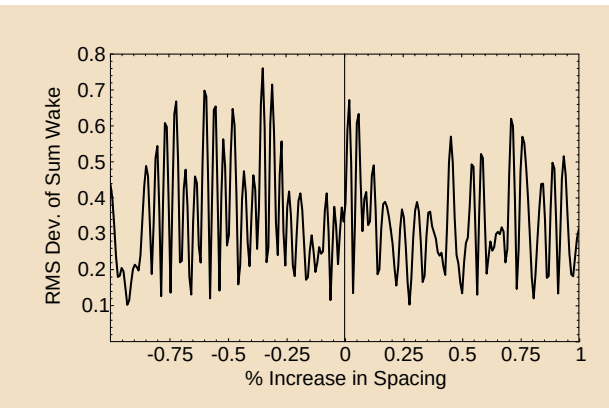

Figure 3: Sum Wake with Q ~ Q_{copper}

our structures. However, at ~-0.35% there is a peak value (~0.76 V/pC/mm/m) and should there be a systematic error in the cell frequencies then this value will result. In order to understand the effects of this error the multi-bunch beam train was tracked through 5,000 or so linacs all perfectly aligned and with a beam intially offset by

1μm from the axis of the linac. The resulting emittance and phase space are shown in Fig. 4 and 5, respectively and it is evident that little emittance dilution occurs

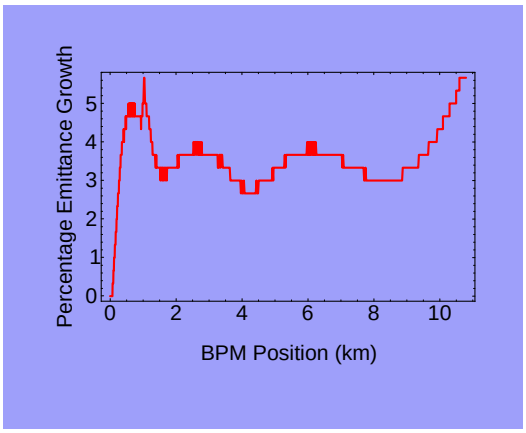

Figure 4: Emittance Growth for Q ~ Q_{copper}

~6%) and the particles are well contained within the normalised circle in phase space.

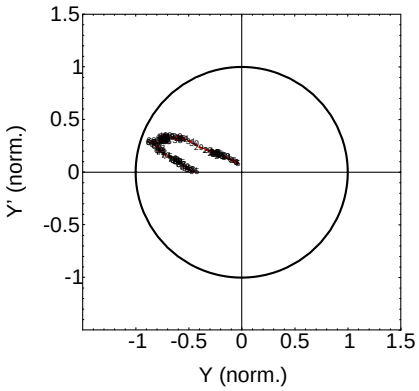

Figure 5: Phase Space for Q ~ Q_{copper}

If we damp the manifold very heavily (with a Q of ~ 200) then the wakefield is affected dramatically (see Fig. 6).

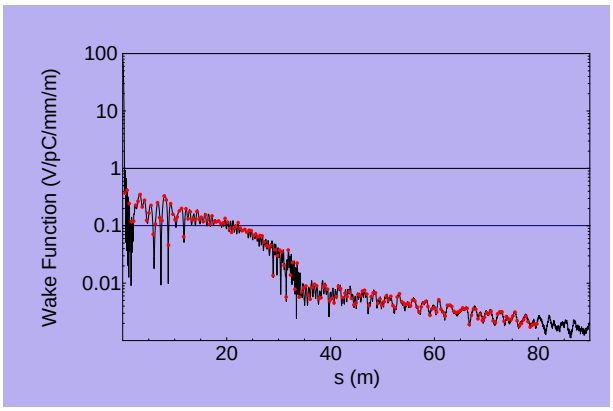

Figure 6: Envelope of Wake Function for Q ~200

The tilt in the envelope of the wakefield occurs entirely due to the loading of the manifold. Further, the sum wakefield is reduced by a factor of 3 or more and hence it is to be expected that little emittance growth will occur under these conditions. Indeed, tracking through 11km of accelerator (at a bunch spacing of 0.45% which achieves a maximum sum wakefield of 0.35 V/pC/mm/m) reveals that zero emttance dilution now occurs as a result of long-range transverse wakefields and the particles are well contained within phase space (see Fig. 7). It is interesting

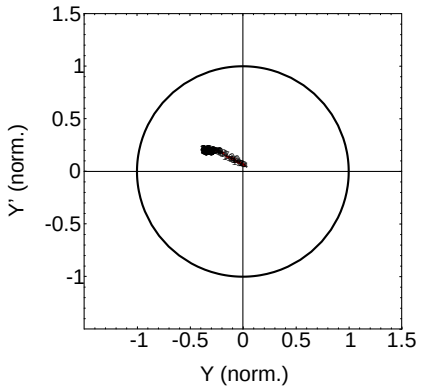

Figure 7: Phase Space for Q ~200

to note that the character of the resonances in the sum wakefield changes in the presence of heavy damping and as the damping is reduced the original functional form, shown in Fig 3, is reproduced. Reducing the damping to Q ~ 800 results in a maximum sum wakefield of ~ 0.56 V/pC/mm/m and this occurs at the same location as that of the purely copper damped manifold (at 0.35% of the nominal bunch spacing). The emittance dilution that occurs is ~ 2%.

4 DISCUSSION

The present RDDS1 accelerator meets the NLC specifications for a 1.5 TeV collider. Furthermore, any errors that occurs in fabricating the structure [6] may be compensated for by adding damping to the four manifolds.

REFERENCES

[1] N.M. Kroll, "The SLAC Damped Detuned Structure: Concept and Design", PAC97, Vancouver, May 1997

[2] R.M. Jones et al, "Equivalent Circuit Analysis of the SLAC DDS" EPAC'96, Sitges, June 1999

[3] R.M. Jones et al, "Including Cell Losses in the Equivalent Circuit Model of The SLAC DDS", PAC99. N.Y.C., March 1999

[4] R.M. Jones et al, "Applications of the Mapping Function Technique to the Design of Damped Detuned Structures and to the Rapid Calculation of their Wakefields", PAC97, Vancouver, May 1997

[5] J.W. Wang et al, "Design, Fabrication and Measurement of the First RDDS", LINAC2000

[6] R.M. Jones et al, this conf., EPAC2000, Vienna, 2000